Thermodynamic effects of proline introduction on protein stability

ARTICLE *in* PROTEINS STRUCTURE FUNCTION AND BIOINFORMATICS · FEBRUARY 2006

Impact Factor: 2.63 · DOI: 10.1002/prot.21215 · Source: PubMed

9 AUTHORS, INCLUDING:

Mili Das
Nirma University
12 PUBLICATIONS **144** CITATIONS
SEE PROFILE

Minhajuddin Sirajuddin
University of California, San Francisco
8 PUBLICATIONS **526** CITATIONS
SEE PROFILE

Sankaranarayanan Srinivasan
Baylor College of Medicine
10 PUBLICATIONS **162** CITATIONS
SEE PROFILE

PROTEINS: Structure, Function, and Bioinformatics 66:480–491 (2007)

Thermodynamic Effects of Proline Introduction on Protein Stability

Ravindra Singh Prajapati,[1] Mili Das,[1] Sridhar Sreeramulu,[1] Minhajuddin Sirajuddin,[1] Sankaranarayanan Srinivasan,[1] Vaishnavi Krishnamurthy,[1] Ranganathan Ranjani,[1] C. Ramakrishnan,[1] and Raghavan Varadarajan[1,2]*

[1]*Molecular Biophysics Unit, Indian Institute of Science, Bangalore 560 012, India*
[2]*Chemical Biology Unit, Jawaharlal Nehru Center for Advanced Scientific Research, Jakkur, P.O., Bangalore 560 004, India*

ABSTRACT **The amino acid Pro is more rigid than other naturally occurring amino acids and, in proteins, lacks an amide hydrogen. To understand the structural and thermodynamic effects of Pro substitutions, it was introduced at 13 different positions in four different proteins, leucine–isoleucine–valine binding protein, maltose binding protein, ribose binding protein, and thioredoxin. Three of the maltose binding protein mutants were characterized by X-ray crystallography to confirm that no structural changes had occurred upon mutation. In the remaining cases, fluorescence and CD spectroscopy were used to show the absence of structural change. Stabilities of wild type and mutant proteins were characterized by chemical denaturation at neutral pH and by differential scanning calorimetry as a function of pH. The mutants did not show enhanced stability with respect to chemical denaturation at room temperature. However, 6 of the 13 single mutants showed a small but significant increase in the free energy of thermal unfolding in the range of 0.3–2.4 kcal/mol, 2 mutants showed no change, and 5 were destabilized. In five of the six cases, the stabilization was because of reduced entropy of unfolding. However, the magnitude of the reduction in entropy of unfolding was typically several fold larger than the theoretical estimate of -4 cal K^{-1} mol^{-1} derived from the relative areas in the Ramachandran map accessible to Pro and Ala residues, respectively. Two double mutants were constructed. In both cases, the effects of the single mutations on the free energy of thermal unfolding were nonadditive. Proteins 2007;66:480–491.**

Key words: thermostability; protein engineering; entropy; unfolded state and conformational flexibility

INTRODUCTION

Modification of protein stability through mutation is the goal of several protein engineering studies. Approaches to enhance protein stability include introduction of favorable electrostatic interactions,[1,2] filling in of interior cavities,[3,4] and removal of unfavorable electrostatic interactions.[5] Another approach to increase protein stability is to decrease the conformational entropy of the denatured state. This can most obviously be achieved by introduction of Cys residue pairs at positions compatible with disulfide bond formation in the folded state of the protein.[6,7] However, formation of disulfides does not readily occur in the reducing environment of the cytoplasm. Proteins with multiple disulfides are typically difficult to express in soluble form in *E. coli*. An alternative method to decrease the conformational entropy of the denatured state is by introduction of the rigid residue Pro. Unlike other residues, the ϕ main chain dihedral angle of Pro is constrained to $-63 \pm 15^{\circ}$[8] because of the presence of the pyrrolidene ring. Pro residues in proteins also lack an amide hydrogen. Conserved Pro residues are important for protein stability.[9] As with disulfides, introduction of the rigid residue Pro into a protein sequence is expected to decrease the conformational entropy of the denatured state and consequently lead to protein stabilization. Consequently, there have been previous attempts to increase protein stability by introduction of Pro residues. However, these have had varying results with stabilization observed in some cases and destabilization in others.[10–14] It is therefore currently unclear whether or not introduction of Pro at a given position in a protein structure will be stabilizing and whether such stabilization effects are temperature dependent.

Abbreviations: LIVBP, leucine–isoleucine–valine binding protein; MBP, maltose binding protein; RBP, ribose binding protein; Trx, *E. coli* thioredoxin; GdmCl, guanidinium chloride; DSC, differential scanning calorimetry; CGH10, citrate 10 m*M*, glycine 10 m*M*, HEPES 10 m*M*; WT, wild type; CNS, crystallography and NMR system; RMSD, root mean square deviation.

The Supplementary Material referred to in this article can be found at http://www.interscience.wiley.com/jpages/0887-3585/suppmat/

Grant sponsor: Department of Biotechnology and Department of Science and Technology, Government of India.

*Correspondence to: Raghavan Varadarajan, Molecular Biophysics Unit, Indian Institute of Science, Bangalore, 560 012, India. E-mail: varadar@mbu.iisc.ernet.in

Received 23 January 2006; Revised 6 June 2006; Accepted 2 August 2006

Published online 10 October 2006 in Wiley InterScience (www.interscience.wiley.com). DOI: 10.1002/prot.21215

With recent advances in genomic sequencing technology and the availability of information on single nucleotide polymorphisms, it is also important to be able to predict the effects of nonsynonymous single nucleotide polymorphisms on protein structure, stability, and function.[15,16] We have therefore studied the structural and thermodynamic effects of introducing Pro at 13 different positions in four different proteins from *E. coli*. The four proteins are leucine–isoleucine–valine binding protein (LIVBP), maltose binding protein (MBP), ribose binding protein (RBP), and thioredoxin (Trx). The first three proteins are relatively large (344, 370, and 271 amino acids in length, respectively), monomeric, two domain proteins found in the periplasm of *E. coli*. They are involved in binding and transport of leucine/isoleucine/valine, maltose, and ribose, respectively. Trx is a 108 amino acid long, cytoplasmic, disulfide oxidoreductase. The four proteins were chosen because they could be expressed to high levels in *E. coli*, showed reversible thermal and chemical denaturation, and crystal structures of the WT protein are available. Stabilities were studied as functions of pH, temperature, and chemical denaturant concentration. The results show that the mutations can be accommodated without structural distortion of the protein. The mutants did not show enhanced stability with respect to chemical denaturation at room temperature. However, 6 of 13 single mutants and 1 of 2 double mutants showed small but significant increases in the thermal stability. The thermodynamic and structural data were analyzed to derive guidelines for selection of structurally compatible sites for introduction of Pro residues in proteins.

MATERIALS AND METHODS

Mutagenesis, Expression, and Protein Purification

All mutants were constructed by site directed mutagenesis following the Stratagene Quik-Change protocol as described previously[17] except the single mutants V86P and A108P as well as the double mutant (D2P,A108P) of *E. coli* Trx. V86P and A108P were constructed by an overlap PCR strategy.[17] All mutations were confirmed by DNA sequencing as well as mass spectroscopy (ESI-MS) for purified proteins. The double mutant (D2P,A108P) was constructed by subcloning the RsrII-HindIII fragment containing the A108P mutation from pBAD24TrxA(A108P) into pET20b(+) TrxAD2P.

The malE (MBP) gene cloned in the vector pMALp2MBP[18] was used as a template for mutagenesis. K34P, D41P, Q78P, D82P, D287P, and V357P single mutants as well as a double mutant (D287P,V357P) were constructed. WT and mutant proteins were expressed in the *E. coli* strains DH5α and Pop-6590 (ΔmalE), respectively, by inducing the cell culture with 0.1 m*M* IPTG as described.[19,20] WT and mutant proteins were isolated by following osmotic shock as described previously.[19]

The rbsB gene (RBP) cloned in plasmid pCMB1 (a gift from S. Mowbray) was used as the template for mutagenesis. A mutant K270P was constructed. Mutant protein was expressed in the deletion strain Mri7 (ΔrbsB)[21] and WT in strain DH5α. Cells were grown in LB medium containing 100 mg/L ampicillin at 37°C and induced with 0.1 m*M* IPTG at an OD_{600} of 0.8. After 6 hr incubation at 37°C, cells were pelleted at 6000 rpm. Following osmotic shock[22] the protein was further purified by ion-exchange chromatography on a Q-sepharose fast flow column using a 0–0.4*M* NaCl gradient in 10 m*M* Tris buffer pH 8 at 4°C.

Plasmid pJSty (a gift from L. Luck) expressing LIVBP under control of the T7 promoter was used for mutagenesis. D2P and K43P mutants were constructed. WT and mutant proteins were expressed in BL21 (DE3) *E. coli* bacterial strain. Protein was isolated and purified by a similar procedure as described above for RBP.

The TrxA gene was cloned in vectors pBAD24 and pET20b(+) for overexpression under control of the P_{BAD} and *T7* promoters, respectively. Single mutants D2P, V86P, V91P and the double mutant (D2P,A108P) present in the pET20b(+) TrxA plasmid were expressed in BL21(DE3) without induction as this plasmid showed leaky expression. Mutant A108P in plasmid pBAD24TrxA was expressed in the *E. coli* strain DH5α following induction of the cell culture with 0.2% arabinose. Following chloroform shock, WT and mutant Trx proteins were isolated as described previously.[23] Protein purity was assessed by Coomassie staining following SDS-PAGE. All the proteins were ≫95% pure. Protein concentrations were estimated using extinction coefficients of 35600, 65370, 4350, and 13700 M^{-1} cm^{-1} at 280 nm for LIVBP, MBP, RBP, and Trx, respectively. The extinction coefficients of LIVBP and RBP were calculated as described previously[24] and those of MBP and Trx were identical to those described previously.[19,25] RBP lacks Trp residues and therefore has a small extinction coefficient.

CD Measurement

CD Spectra of WT LIVBP, MBP, RBP, and their mutant proteins were acquired in buffer CGH 5 (Citrate, HEPES, and Glycine 5 m*M* of each) at pH 7, and for WT and mutant Trx in 10 m*M* phosphate buffer pH 7 on a Jasco J-715 CD spectrometer. Wavelength scans from 200 to 250 nm for 5–8 μ*M* proteins were performed in a 0.1 cm path length cuvette using a slit width of 1 nm and a scan rate of 20 nm/min. All spectra were acquired at 298K.

Isothermal Equilibrium Unfolding of LIVBP, MBP, RBP, and Trx

Isothermal urea denaturation studies of LIVBP, MBP, RBP, and their mutants were carried out in CGH10 buffer containing 150 m*M* KCl at pH 7, 298K as described previously.[19,26] Isothermal GdmCl denaturation studies of Trx and its mutants were carried out as described previously[27] in 50 m*M* phosphate buffer at pH 7, 298K. Denaturation was monitored using fluorescence on a Fluoro-Max3 fluorimeter. Protein concentrations of

TABLE I. Structural Parameters at Sites of Pro Mutants of LIVBP, MBP, RBP, and Trx in the Wild Type Protein and Thermodynamic Parameters for Mutants

Mutants	Short contacts[a]	ϕ (°)	ψ (°)	Accessibility of WT residue, %	Secondary structure[b]	ΔT_m (°C)[c]	ΔC_m (M)[c]	B/B-average[d]
LIVBP								
D2P	5	−129.0	136.0	16.3	O (1–2)	−0.4	−0.6	1.9
K43P	0	−86.0	149.0	25.0	βS (43–51)	1.0	−0.1	1.0
MBP								
K34P	0	−80.2	134.7	55.5	βS (34–38)	2.2	0.0	1.3
D41P	0	−67.5	135.4	79.1	O (39–42)	0.3	0.0	1.3
E78P	0	−74.1	139.9	54.3	O (78–82)	−0.9	−0.2	1.2
D82P	0	−84.3	167.7	65.0	O (78–82)	0.0	−0.1	1.3
D287P	0	−54.9	−40.0	40.5	H (287–296)	0.7	0.0	0.9
V357P	1	−64.3	−49.4	11.6	H (357–369)	0.6	−0.5	1.4
D287P, V357P	—	—	—	—	—	0.1	−0.3	
RBP								
K270P	1	−70.0	121.0	30.1	O (269–271)	−2.3	0.0	0.7
Trx								
D2P	2	−67.0	−17.0	86.5	O (1–4)	0.7	0.1	1.1
V86P	0	−70.0	126.0	35.1	βS (85–92)	−2.9	−0.3	0.7
V91P	1	−102.0	102.0	50.2	βS (85–92)	−4.7	−0.6	0.7
A108P	0	−106.0	999.0	132.9	O (105–108)	0.5	0.0	2.3
D2P, A108P	—	—	—	—	—	3.1	0.1	

[a]Short contacts of the modeled mutated residue with surrounding residues in the wild type protein.
[b]Secondary structure abbreviations: H, helix; βS, beta strand; O, others. The numbers in parentheses are the residue numbers indicating the first and last residues in that particular element of secondary structure.
[c]ΔT_m and ΔC_m are the changes in the midpoints of thermal and chemical denaturation, respectively, relative to WT.
[d]Ratio of B-factor of WT residue to the average B-factor of all atoms in the protein.

3 μ*M*, 0.5 μ*M*, 8 μ*M*, and 5 μ*M* for LIVBP, MBP, RBP, and Trx were used, respectively. Proteins were incubated in denaturant for 5 hr at 25°C. This time was sufficient to attain equilibrium as monitored by the time independence of the fluorescence intensity. Longer incubation times (up to 10 hr) did not result in any changes in the measured stability parameters. The denaturant concentration was estimated by refractive index measurements. Unfolding was monitored by measuring fluorescence at 323, 337, 303, and 338 nm for LIVBP, MBP, RBP, and Trx, respectively, and all the proteins were excited at 280 nm. Values of the parameters ΔG° and m were estimated according to the linear free energy model as described previously.[28] All the data were analyzed by using Sigma Plot.

Thermal Denaturation

Thermal denaturation for WT and mutant proteins was carried out by using the Microcal VP-DSC. DSC measurements were carried out as a function of pH in CGH10 buffer, in the pH range 6–10, using protein concentrations of 0.2–0.5 mg/mL. Protein solutions used for the DSC study were degassed before loading into the microcalorimeter, and the pH was adjusted manually before degassing. A scan rate of 90°C/hr was used for MBP, RBP, LIVBP and 60°C/hr for Trx as described previously.[19,27] DSC scans were carried out from 25°C to 85°C for LIVBP, MBP, RBP and 25°C to 110°C for Trx. The reversibility of thermal unfolding was confirmed by carrying out a rescan at each pH before removing sample from the calorimeter. DSC data were fit to a two-state unfolding with baseline subtraction model using the Origin DSC software provided by Microcal Inc.

Crystallization, Data Collection, and Refinement

Wild type MBP has earlier been reported to crystallize by the hanging drop method using polyethyleneglycol 20000 (PEG 20K) in 20 m*M* MES buffer, pH 6.2.[29] Our attempts to crystallize MBP under these reported conditions yielded no results. Hence, we screened crystallization conditions for wild type MBP using the crystal screens 1 and 2 of Hampton Research. Diffraction quality crystals were obtained under previously unreported conditions with PEG 400. Crystallization was then set up for the wild type as well as mutant MBPs under these conditions using the hanging drop vapor diffusion method. The reservoir solution contained 30% PEG 400 (Sigma Chemical) and 0.1*M* $CdCl_2$ in 0.1*M* sodium acetate buffer, pH 4.6. Three microliters of the protein in CGH-10 buffer, pH 7.2, were mixed with 2 μL of the reservoir solution on a siliconized cover slip, inverted and suspended over a well of a 24-well plate, and sealed with vacuum grease. The plates were kept at room temperature (~20°C). The stock protein concentrations used were 11, 14, and 15 mg/mL for D41P, D82P, and D287P, respectively. The wild type as well as the mutants produced crystals of approximate size 0.25 × 0.18 × 0.1 mm^3 under this condition in 6–8 days.

Crystals were mounted in 0.7 mm diameter capillary tubes, and diffraction data were collected using a

MAR300 imaging plate system mounted on a Rigaku RU-200 rotating anode X-ray generator (44 kV, 70 mA) at room temperature. The crystal to plate distance was 120 mm and images were collected for every 1° oscillation with an exposure time of 900 s. The data were processed using DENZO and scaled using SCALEPACK from the HKL program package.[30]

The structure of wild type MBP was solved by molecular replacement using the coordinates of maltotetraitol-bound wild type MBP (PDB ID 1FQA) as the starting model. 1FQA was used as the starting model because it had the same space group and unit cell parameters as those observed for the present crystals.[31] Although 1FQA has bound tetraitol, the protein adopts the open conformation characteristic of ligand free MBP.[29] Molecular replacement was done using the MOLREP program of the CCP4[32] program suite. The structures of the mutants were then solved by molecular replacement using the coordinates of WT as the starting model. The structures were refined using CNS v1.1,[33] and further manual adjustments were made using O. Refinement included positional refinement followed by simulated annealing and finally B-factor refinement. Water molecules were added using the water pick program in CNS. $2f_o - f_c$ and $f_o - f_c$ maps were generated in CNS and contoured at 1.5σ and 3.0σ, respectively. After refinement was completed, the mutant structures were superposed onto the wild type structure using the lsqkab program of the CCP4 program suite and root mean square deviations (RMSD) were calculated. The absolute values of the differences in phi and psi values of each residue between the wild type and mutant were also calculated.

RESULTS

Selection of Sites for Introduction of Pro Residues

Pro residues in a polypeptide chain have restricted ϕ values of $-63 \pm 15°$[8] and also lack a main chain amide hydrogen. To identify locations suitable for introduction of Pro residues, the following criteria were used: (a) The WT residue amide proton should not be involved in a main chain hydrogen bond, (b) introduction of Pro should not lead to steric clashes with other residues in the protein, and (c) the side chain of the WT residue should not be involved in significant stabilizing interactions. A computer program was devised to model Pro residues at each position in a polypeptide of known three dimensional structure. By using an in-house-developed software (details to be published elsewhere), prolyl residues were fixed to the backbone at those residues that have Ramachandran ϕ angles in the neighborhood of −60° with both C^γ endo and exo orientations. The atoms of the proline ring, viz., C^β, C^γ, and C^δ and their associated hydrogen atoms $H^{\beta1}$, $H^{\beta2}$, $H^{\gamma1}$, $H^{\gamma2}$, $H^{\delta1}$, and $H^{\delta2}$ were examined for short contacts with spatial close neighbors in the protein structure using Ramachandran-contact criteria.[34–36] In addition, nonbonded van der Waal's energy of interaction between these atoms and those that occur within a sphere of 4.0 Å was also computed using standard constants.[35] The choice between endoconfigurations and exoconfigurations of C^γ was decided using the following criterion. If both were free of short contacts or if both had short contacts, the one with the lower energy is chosen. On the other hand, if one had short contacts and the other none, the one with no short contacts was preferred. The present software orders the Pro-mutations at the various possible sites, in the order of increasing nonbonded energy arising because of the mutated-prolyl residue so that the best sites can be chosen

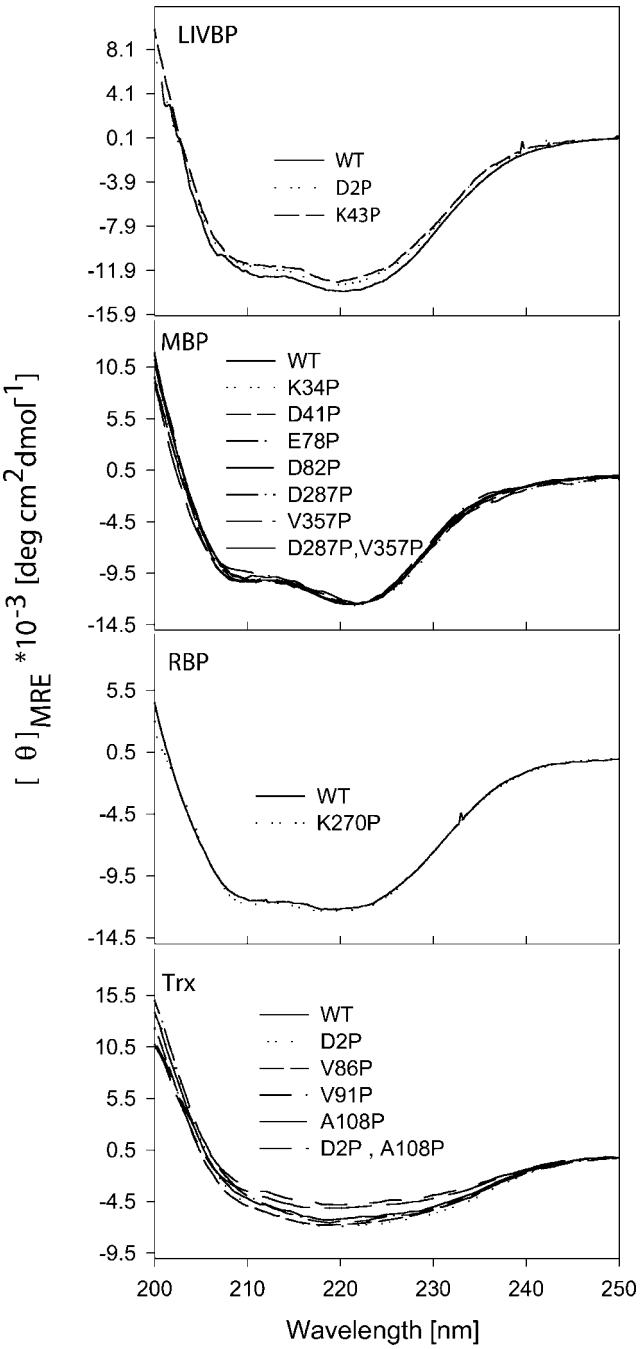

Fig. 1. Far-UV CD spectra for WT and Pro mutants of LIVBP, MBP, RBP, and Trx at pH 7 and 298K.

TABLE II. Summary of Data Collection, Reduction, and Refinement for the WT and Mutant MBPs

Parameter	WT	D41P	D82P	D287P
a (Å)	44.43	44.66	44.57	44.81
b (Å)	65.45	65.79	65.59	65.97
c (Å)	57.93	58.09	58.13	58.15
$\alpha = \gamma$	90.0	90.0	90.0	90.0
β	100.95	100.9	101.1	100.9
R_{merge} (%)	7.7	11.0	10.5	13.1
Resolution (Å)	1.9	1.9	2.0	2.5
Total no. of reflections	78056	52592	76805	19959
No. of unique reflections	24721	24463	22232	10413
Completeness (%)	95.0	94.3	100.0	89.3
No. of water molecules	290	199	276	74
R (%)	21.9	21.9	19.9	20.9
R_{free}(%)	25.9	25.9	25.1	30.5
Backbone RMSD relative to WT (Å)		0.27	0.20	0.26

in conjunction with other criteria described below. The program identified residue positions where Pro could be modeled with reasonable stereochemistry. At such positions the estimated change in ϕ upon Pro substitution ($\Delta\phi$), the number and energetics of unfavorable contacts introduced upon substitution, and the hydrogen bonds/salt bridges formed by the WT residue were calculated. Based on this analysis, 13 different sites in four different proteins were selected for introduction of Pro. Sites were chosen to span a range of $\Delta\phi$ values, secondary structures, and proximity to chain termini. The stereochemical parameters as well as the stability changes observed upon mutation are summarized in Table I.

Characterization of WT and Mutant Proteins

All proteins were purified to homogeneity as judged by SDS-PAGE. Approximate yields of purified WT protein were 20, 25, 40, and 90 mg/L for LIVBP, MBP, RBP, and Trx, respectively. Mutant proteins showed similar levels of expression to the corresponding WT. Fluorescence spectra of WT proteins are shown in (Supplementary Fig. 1) with excitation at 280 nm. LIVBP, MBP, RBP, and Trx contain 3, 8, 0, and 2 Trp residues, respectively. In all cases, there is a red shift upon denaturation. The λmax in the denatured states are 355, 353, 305, and 357 nm for LIVBP, MBP, RBP, and Trx, respectively. All mutants show very similar fluorescence spectra to the corresponding WT (data not shown). Far-UV CD spectra for mutants are also very similar to the corresponding WT (see Fig. 1). The spectroscopic data therefore suggest that in all cases the Pro residue has been accommodated without appreciable changes in the secondary and tertiary structure of the protein. For the D41P, D82P, and D287P mutants of MBP this lack of structural change was confirmed by X-ray crystallography as described below. The functional activity for Pro derivatives of MBP and Trx was checked as described previously,[19,25] and these mutants showed activity similar to the corresponding WT protein (data not shown).

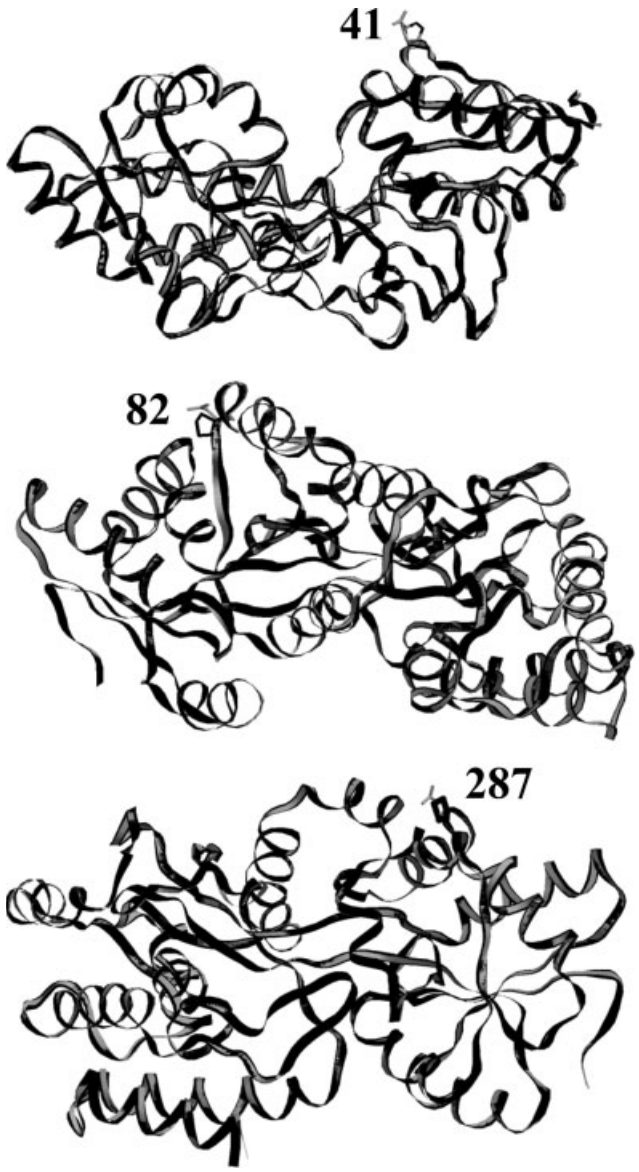

Fig. 2. Superposition of the overall structures of the mutants (black) D41P, D82P, and D287P on the wild type (grey) MBP. The side chains are shown for the residue that has been mutated.

Crystallographic Studies

A new crystal form of unliganded MBP (for both wild type and mutant proteins) was obtained in these studies under conditions that have not been previously reported for MBP. In contrast to the conditions used previously for MBP crystallization[29] no seeding was required under these conditions. The X-ray crystallographic data and refinement parameters for the MBP wild type and mutants are summarized in Table II. All proteins crystallized in the primitive monoclinic space group $P2_1$ and

TABLE III. Structural Parameters for Residues Around the Site of Mutation for the D41P, D82P, and D287P MBP Mutants

Residue no.	Φ (WT)	ΔΦ[a] (°)	Ψ (WT)	ΔΨ[a] (°)	Main chain RMSD[b] (Å)	Side chain RMSD[b] (Å)
40	−64.2	3.1	151.1	2.1	0.14	0.08
41	−69.2	−0.5	145.7	−3.5	0.24	0.22
42	54.5	−2.4	36.8	16.9	0.21	0.08
81	−73.0	6.5	141.6	2.1	0.38	0.30
82	−67.7	5.1	164.8	−15.8	0.40	0.34
83	−57.2	5.6	−34.1	−2.0	0.41	0.67
286	−133.4	−2.7	165.1	−2.7	0.19	0.07
287	−60.1	−4.1	−39.8	11.8	0.25	0.10
288	−70.5	1.2	−38.7	−7.2	0.20	0.13

[a]$\Delta\Phi = \Phi$ (mutant) − Φ(WT), $\Delta\Psi = \Psi$(mutant) − Ψ(WT).
[b]Following superposition using all main chain atoms of the protein, RMSD values were calculated. For the side chain RMSD calculation, atoms only up to the C_β were included for the residue that was mutated.

had similar unit cell parameters. The overall structure was virtually unchanged upon mutation (Fig. 2, Table III). Figure 2 shows the superposed structures. Side chains are shown only at the site of mutation. Supplementary Figures 2, 3, and 4 show the values of ΔΦ, ΔΨ, and main chain RMSD as a function of residue number for all the three mutants. The region around the site of each mutation was unchanged. Most differences occurred either at loops/disordered regions or at the chain termini. Structural parameters around the site of mutation are summarized in Table III. In all cases, the Pro mutation is accommodated with minimal structural change. Figure 3 shows that the structures of all three mutants in the vicinity of the mutation are all very similar to WT MBP.

Chemical Denaturation Studies

Chemical denaturation studies were carried out using either urea (for LIVBP, MBP, RBP) or GdmCl (for Trx). Denaturation was monitored using fluorescence spectroscopy as described in Materials and Methods. In all cases, data were fit to a two-state unfolding model, and free energies of unfolding at zero denaturant were determined using linear extrapolation as described previously.[37] Denaturation of MBP, Trx, and RBP has been shown previously to be two state by coincidence of melts monitored by fluorescence and far UV-CD.[19,26,27] Denaturation of LIVBP is also two state by the same criterion (Supplementary Fig. 5). The results are summarized in Figure 4 and Table IV. Of all the mutants examined in the present study, only the D2P and (D2P,A108P) mutants of Trx are stabilized with respect to chemical denaturation. All other mutants have either identical or slightly lower stability than the corresponding WT. GdmCl was used for the Trx denaturation studies because Trx is relatively insensitive to urea denaturation and proper unfolded baselines could not be obtained in urea. However, even when urea was used as a denaturant the D2P single mutant and the D2P,A108P double mutant transitions occurred at higher urea concentrations than for WT (data not shown).

Thermal Denaturation Studies

Pro mutants are expected to stabilize proteins by decreasing the conformational entropy of unfolding. The total entropy of unfolding, ΔS, can be broken into two components ΔS_{conf} and ΔS_{other}, where ΔS_{conf} is the conformational entropy change upon unfolding and is always positive. Introduction of Pro is expected to decrease the magnitude of ΔS_{conf} and therefore increase the free energy of unfolding ($\Delta G^\circ = \Delta H - T(\Delta S_{conf} + \Delta S_{other})$). If it is assumed that the mutation does not drastically affect ΔS_{other} and ΔH, then $\Delta\Delta G^\circ \approx -T\Delta\Delta S_{conf}$, where $\Delta\Delta G^\circ = \Delta G^\circ$ (mutant) − ΔG° (WT). Hence stabilizing effects due to negative values of $\Delta\Delta S_{conf}$ are likely to be enhanced at higher temperatures. The thermal stabilities for all proteins were characterized by DSC in the pH range 6.0–10.0. At the T_m of unfolding 50% of the molecules are folded and ΔG° (T_m) = 0. The results are summarized in Table I (Supplementary information), and DSC data at neutral pH are shown in Figure 5. Average values of ΔT_m for each mutant are shown in Table I. The following mutants showed small but significant increases in T_m: the K43P mutant of LIVBP; the K34P, D287P, V357P mutants of MBP; the D2P, A108P single mutants as well as the (D2P,A108P) double mutant of Trx. The significance was assessed by carrying out a paired *t*-test for WT and mutant T_m values as a function of pH as described previously.[20] Values of ΔC_p for each protein were estimated from the slope of the linear dependence of ΔH° (T_m) upon T_m. Values of ΔC_p for WT proteins are 5.8 ± 0.6, 5.4 ± 1.9, 4.5 ± 0.2, and 1.2 ± 0.1 kcal mol^{-1} K^{-1} for LIVBP, MBP, RBP, and Trx, respectively (Supplementary Fig. 6). Mutant proteins had ΔC_p values approximately similar to the corresponding WT. The T_m values of the various mutant and WT proteins are different. To compare WT and mutant stabilities at a common temperature, the measured values of ΔH° (T_m) and ΔS (T_m) were extrapolated to a common reference temperature using the measured values of ΔC_p as described previously.[27] For WT and mutant LIVBP, MBP, and RBP this reference temperature was chosen to be 64°C (the average

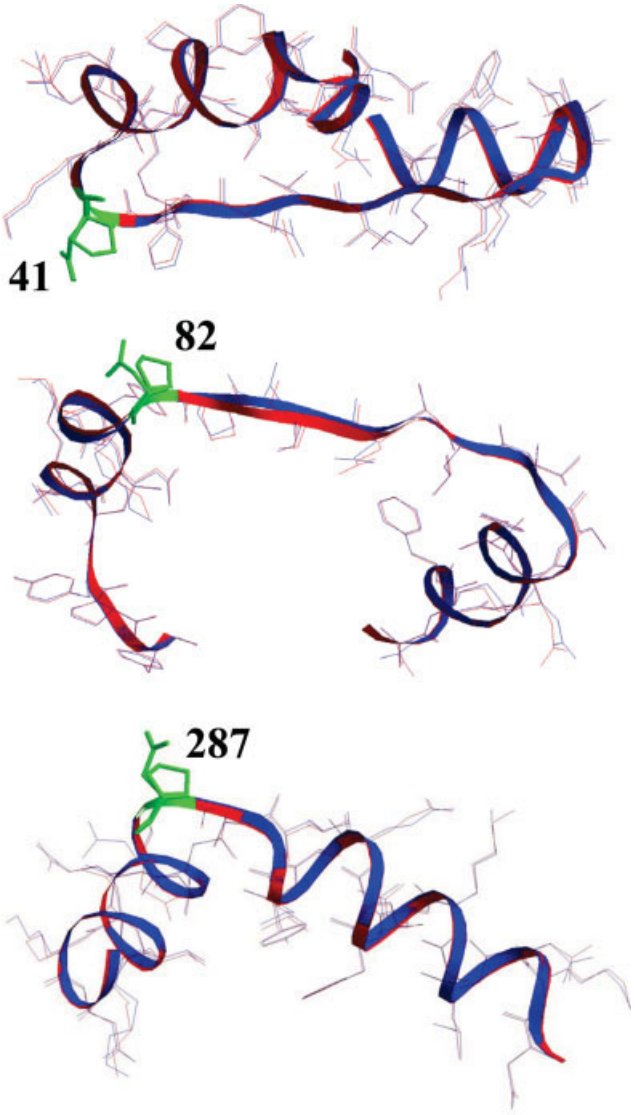

Fig. 3. Superposition of the mutant MBPs on the wild type around the site of mutation. The mutants are shown in red while the wild type is shown in blue. The residue at which mutation occurs is shown in green. Residues 24–58, 65–92, and 272–297 are shown for the D41P (top), D82P (middle), and the D287P (bottom) mutants, respectively.

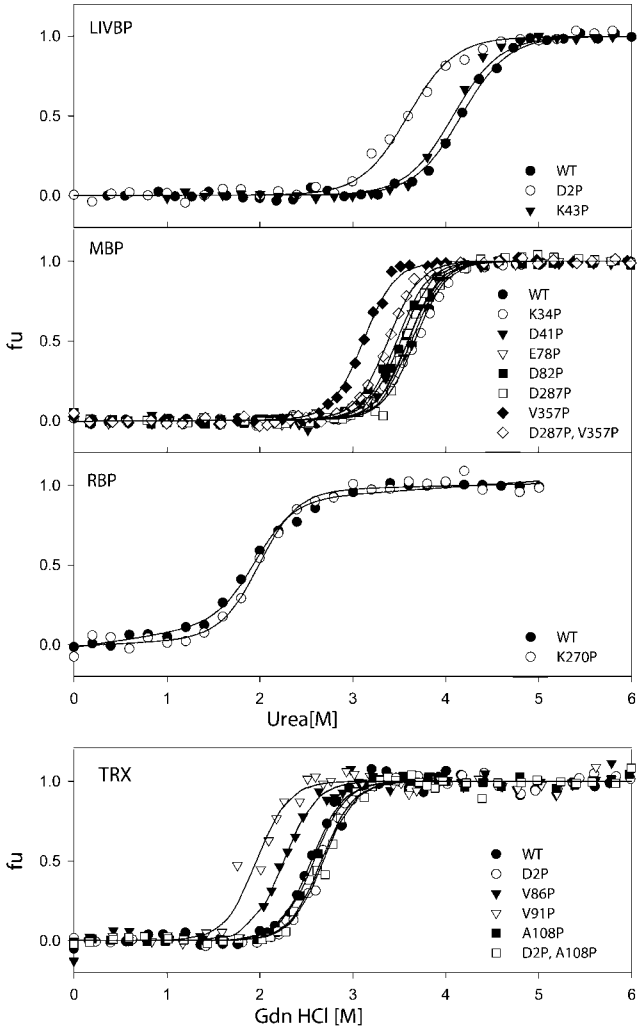

Fig. 4. Isothermal chemical denaturation curves at pH 7, 298K for Pro mutants of LIVBP, MBP, RBP, and Trx. Protein denaturation was monitored by protein fluorescence as described in the text. The fraction of unfolded protein (fu) is plotted as a function of denaturant concentration.

T_m of the three WT proteins at pH 7.0). For WT and mutant Trx, the reference temperature was chosen to be the T_m of WT Trx at pH 7.0 (87.8°C). Values of changes in thermodynamic parameters at the reference temperature for each mutant, relative to the corresponding WT, are summarized in Table V. In most Pro mutants that show thermal stabilization, as expected, this is because of a reduced entropy of unfolding. The only exception to this is the K43P mutant of LIVBP, where stabilization is enthalpy rather than entropy driven. The measured values of ΔH° (T_m) and ΔS (T_m) were not extrapolated to room temperature, because of the large errors involved in such extrapolation.[19,38]

DISCUSSION

Effect of Mutations on Room Temperature Stability

A summary of the structural characteristics of each site chosen for mutation as well as the changes in C_m and T_m associated with each mutation is shown in Table I. In four single mutants (LIVBP D2P, MBP V357P, Trx V81P, and Trx V91P), there was an appreciable decrease in C_m upon mutation. In only two cases, the D2P single mutant and the (D2P,A108P) double mutant of Trx a small but significant increase in C_m of 0.1*M* was observed (Table IV, Fig. 4). In all other cases, there were either no or a small decrease in C_m. Thus, the majority of Pro mutants studied here were either neutral or mildly destabilizing with respect to their room temperature stabilities, measured by chemical denaturation. We consider various factors that may contribute to this observation.

TABLE IV. Unfolding Thermodynamic Parameters Obtained From Isothermal Denaturation Studies at pH 7, 298K for WT, and Pro mutants of LIVBP, MBP, RBP, and Trx

Protein	ΔG° (kcal/mol)	$-$m (kcal/mol/M)	C_m[a] (M)	$\Delta\Delta G^\circ$ (kcal/mol)	ΔC_m[a] (M)
LIVBP					
WT	9.8 ± 0.4	2.4 ± 0.1	4.0	—	—
D2P	8.5 ± 0.3	2.4 ± 0.1		−1.3 ± 0.5	−0.6
K43P	9.6 ± 0.3	2.4 ± 0.1		−0.2 ± 0.5	−0.1
MBP					
WT	12.6 ± 0.3	3.5 ± 0.1	3.6	—	—
K34P	12.7 ± 0.3	3.5 ± 0.1		0.1 ± 0.4	0.0
D41P	12.4 ± 0.2	3.5 ± 0.1		−0.2 ± 0.4	0.0
E78P	12.0 ± 0.2	3.5 ± 0.1		−0.6 ± 0.4	−0.2
D82P	12.2 ± 0.2	3.5 ± 0.1		−0.4 ± 0.4	−0.1
D287P	12.5 ± 0.2	3.5 ± 0.1		−0.1 ± 0.4	0.0
V357P	10.8 ± 0.2	3.5 ± 0.1		−1.8 ± 0.3	−0.5
D287P, V357P	11.7 ± 0.2	3.5 ± 0.1		−0.9 ± 0.3	−0.3
RBP					
WT	5.9 ± 0.4	3.0 ± 0.2	2.0	—	—
K270P	6.0 ± 0.4	3.0 ± 0.1		0.1 ± 0.5	0.0
Trx					
WT	8.7 ± 0.3	3.4 ± 0.1	2.5	—	—
D2P	9.0 ± 0.4	3.4 ± 0.1		0.3 ± 0.5	0.1
V86P	7.7 ± 0.3	3.4 ± 0.1		−1.0 ± 0.5	−0.3
V91P	6.7 ± 0.3	3.4 ± 0.1		−2.0 ± 0.4	−0.6
A108P	8.7 ± 0.3	3.4 ± 0.1		0.0 ± 0.5	0.0
D2P, A108P	9.1 ± 0.4	3.4 ± 0.1		0.4 ± 0.5	0.1

For Trx GdmCl was denaturant, and for all other proteins it was urea.
[a]From the multiple experiments, approximate errors in C_m and ΔC_m are estimated to be 0.05*M* and 0.07*M*, respectively.

Structures of the three MBP mutants (see Fig. 3) demonstrate that the Pro residue is accommodated with minimal structural perturbation. Hence, the lack of observed stabilization is unlikely to be due to unfavorable sterics in the native state of the protein. However, it is possible that the introduced Pro residue is not as well packed against its neighbors in comparison with the WT residue.

In addition, a small fraction of each Pro residue will occur in the cis conformation, thus increasing the number of conformations in the denatured state. This proportion depends on the residue preceding Pro and is largest for aromatic amino acids.[39] However, none of the Pro residues in this study was preceded by an aromatic amino acid and this effect will therefore be small. Even a 20% population of a cis Pro in the denatured state will result in a decrease in free energy of the denatured state of about 0.1 kcal/mol ($-$RT ln 1.2).

Another possible factor is that the magnitude of the reduction in conformational entropy of the denatured state due to introduction of Pro may be smaller than the value of -4 cal K^{-1} mol^{-1} estimated previously.[40] The above estimate was derived by considering the relative areas accessible to Ala and Pro in the Ramachandran map.[34] Recent calculations have shown that steric exclusion from non-nearest neighbors can restrict allowed conformations even in a poly-Ala chain.[41] Hence introduction of Pro will result in a smaller magnitude of chain entropy decrease than that estimated from Ramachandran map areas. Other effects such as local structure, compaction of the denatured state, and changes in solvent mobility due to mutation may also modulate the stabilizing effects of the mutation.

Thermal Denaturation Studies

In contrast to the situation at room temperature, several of the Pro mutants appear to show slightly enhanced thermal stability. Six of the 13 single mutants showed statistically significant values of ΔT_m, ranging from 0.1 to 3.1°C, two showed no change, and five were destabilized. Two double mutants were characterized MBP D287P,V357P and Trx D2P,A108P. In both cases, the two mutated residues were far apart in the native structure of the protein and the effects on chemical denaturation were approximately additive, within experimental error. However, for thermal denaturation, the effects were nonadditive. Since introduction of Pro is thought to reduce the conformational entropy of the denatured state, the nonadditivity could be due to some degree of cooperative structure formation in the thermally denatured state. Values of $\Delta\Delta G^\circ$ for each mutant (relative to the corresponding WT) are summarized in Table V. Values of $\Delta\Delta G^\circ$ ranged from -3.2 to $+2.4$ kcal/mol, but the majority of the values were positive, consistent with the positive values of ΔT_m. The values of $\Delta\Delta S$ for almost all Pro mutants were negative. This is

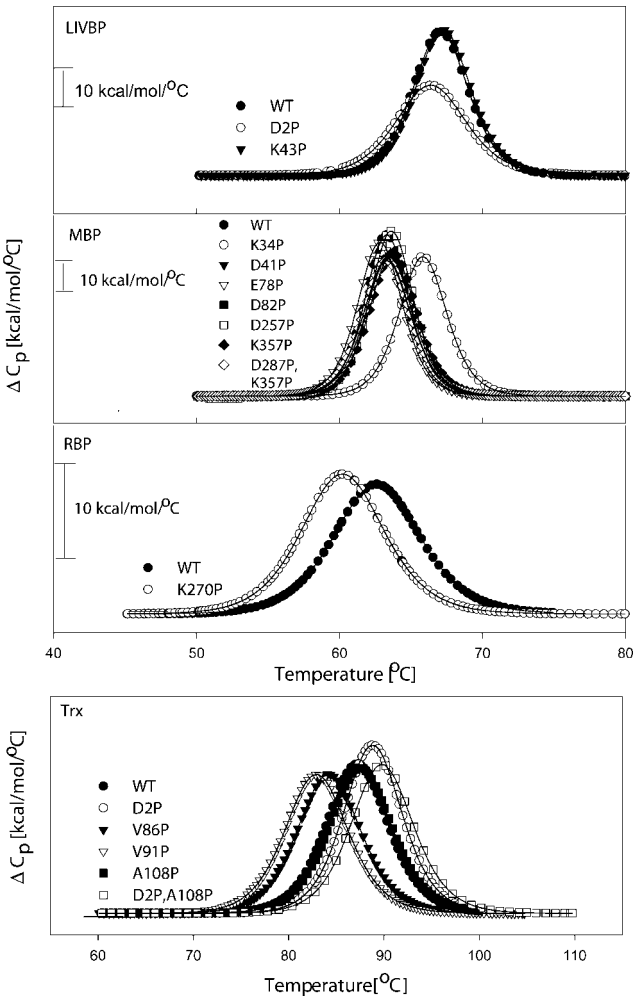

Fig. 5. Baseline subtracted DSC scans for Pro mutants of LIVBP and MBP at pH7.5 and for RBP and Trx at pH 7. The scan rate was 90°C/hr for LIVBP, MBP, RBP, and their mutants and 60°C/hr for Trx and its mutants. Data points are shown as symbols and two-state fits to the data are shown as thin solid lines.

consistent with Pro causing a decrease in the entropy of the unfolded state. However, the magnitude of $\Delta\Delta S$ was appreciably larger than the theoretical estimate of -4 cal K^{-1} mol^{-1}, indicating that other factors are also contributing to $\Delta\Delta S$. In several cases, values of $\Delta\Delta H^\circ$ for such stabilized mutants are large and negative. This is either because of poorer packing in the native state of the mutants or more favorable interactions in the corresponding unfolded state.

Rationalization of Mutant Stability Changes in Terms WT Structural Parameters

The two mutants (Trx D2P and Trx D2P, A108P) that showed an increase in stability with respect to chemical denaturation also showed increased thermal stabilities. In a few cases, despite a significant decrease in stability toward chemical denaturation ($\Delta\Delta G^\circ < -1$ kcal/mol), the thermal stability showed either little change (LIVBP D2P) or was increased (MBP V357P). Residue D2P in LIVBP has a ϕ value of -129° (significantly different from the mean ϕ of -63° for Pro) and the modeled Pro forms several short contacts with its surroundings. Since the residue is close to the N-terminus, it is possible that at higher temperatures, increased conformational flexibility in the native state alleviates the destabilizing effect of the mutation. In MBP, residue 357 is located at the N terminus of a helix adjacent to a turn. Here again, a modeled Pro at this position has a single unfavorable contact which is probably alleviated by increased conformational flexibility of the turn (residues 352–356) at high temperature. Two other mutants, Trx V86P and TrxV91P, are destabilized and have values of $\Delta\Delta G^\circ < -1$ kcal/mol for both chemical and thermal denaturation. Both residues are located within a β-strand (residues 85–92) of Trx. The modeled structure of V91P has a single close contact with its surroundings and also the WT residue has a ϕ value of -102° which may account for the destabilization observed in this mutant. It is not obvious why the V86P mutation should be destabilizing. In this case, the modeled Pro does not form any unfavorable contacts and the WT residue has a ϕ value of -70°, close to the typical value of -63° for Pro. It is possible that the surface packing interactions of the WT residue are more favorable than for the Pro, and this is the cause of the reduced stability. This residue has a low B-factor in WT MBP (Table I). Attempts were also made to look for correlations between the value of ΔT_m and the B-factor of the residue to be mutated, relative to the average B-factor of all atoms of the protein (Table I). Five out of eight positions that had higher than average B-factors showed an increase in thermal stability, one (MBP D82P) showed no change, and two (LIVBP D2P, MBP E78P) showed decreased thermal stability. Three out of four positions that had lower than average B-factors showed decreased thermal stability. B-factors are a measure of residue mobility.

Guidelines for Selection of Sites for Introducing Pro

Pro can be more easily accommodated at positions of higher than average mobility, where rearrangements to accommodate the rigid Pro residue can take place at minimal energetic cost. In addition, the data in Table I suggest that for sites where Pro is to be introduced, it is desirable that the ϕ value is within 20–30° of -63° (the average value for Pro). Larger deviations are permissible close to chain termini. Pro appeared to be well tolerated in turns and coils as well as at the N termini of α-helices and β-strands. However, at nonterminal regions of β-strands (Trx V86P and V91P), it is appreciably destabilizing. At all sites chosen, the WT proton was not involved in a main chain hydrogen bond and the side-chain of the WT residue was not involved in local stabilizing interactions. If we eliminate residues with greater than two predicted short contacts (Table I) or those in the interior of β-strands from the analysis, then of the

TABLE V. Changes in Thermodynamic Unfolding Parameters at pH 7 for Pro Mutants of LIVBP, MBP, RBP, and Trx, Respectively, Relative to Wild Type at the Reference Temperature

Protein	$\Delta\Delta H^\circ$ (kcal/mol)	$\Delta\Delta S$ (cal/mol/K)	$T\Delta\Delta S$ (kcal/mol)	$\Delta\Delta G^\circ$ (kcal/mol)	ΔT_m[a] (°C)
LIVBP					
D2P	−3.9	−10.6	−3.6	−0.3	−0.4
K43P	17.3	47.2	15.9	1.4	1.0
MBP					
K34P	−16.1	−54.8	−18.5	2.4	2.2
D41P	−4.4	−12.8	−4.3	−0.1	0.3
E78P	1.5	10.8	3.6	−2.1	−0.9
D82P	−8.1	−24.3	−8.2	0.1	0.0
D287P	−1.2	−5.6	−1.9	0.7	0.7
V357P	−5.9	−19.2	−6.5	0.6	0.6
D287P, V357P	−12.1	−35.4	−11.9	−0.2	0.1
RBP					
K270P	8.1	27.7	9.3	−1.2	−2.3
Trx					
D2P	−0.3	−2.6	−0.9	0.6	0.7
V86P	0	5.8	2.1	−2.1	−2.9
V91P	6.9	28	10.1	−3.2	−4.7
A108P	−0.8	−3.1	−1.1	0.3	0.5
D2P, A108P	−5.8	−20.5	−7.4	1.6	3.1

For all derivatives of LIVBP, MBP, and RBP, the reference temperature was chosen to be 337.15K, and for Trx derivatives it was 360.95K.
[a]Average ΔT_m values. ΔT_m values as a function of pH for each protein are shown in Table I (Supporting Information). The mean error in ΔT_m is 0.14°C.

TABLE VI. Thermodynamic Parameters Obtained From the Protherm Database[38]

Secondary structure	ΔΔG (kcal/mol) (no. of examples)	Average ΔT_m (°C) (no. of examples)
Helix (total)	−0.7 (23)	−4.5 (18)
Helix (N-terminal residue)	0.5 (12)	0.1 (9)
Helix (Non N-terminal residues)	−2.0 (11)	−9.1 (9)
Random coil	−0.2 (7)	−2.0 (11)
Turn	−0.3 (2)	1.0 (4)
beta sheet	−5.1 (1)	— (0)

Data were classified on the basis of location of the mutation in each secondary structure of the protein. ΔΔG and ΔT_m were averaged for each secondary structure.

10 remaining single mutants, 6 are thermally stabilized, 2 show no change, and 2 are destabilized. Hence these results serve as useful guidelines to select sites for Pro introduction in proteins.

Comparisons With Earlier Studies

There have been several previous studies of Pro mutants of proteins, though none of them are as detailed as the present work. The majority of these studies typically involve a few mutants of a single protein and no thermodynamic or crystallographic data are generally reported. Instead, inactivation times at a reference temperature (which differs from one study to another) are indicated.[42–44] An examination of the Protherm database[45] [http://gibk26.bse.kyutech.ac.jp/jouhou/Protherm/protherm.html] was made for single mutants where a Pro residue was introduced at an exposed site (accessibility $\gg$15%) and for which either information on $\Delta\Delta G$ or ΔT_m was available. The resulting dataset consists of 44 mutants of 14 proteins and the data are summarized in Table II (Supporting Information). Average values of ΔT_m and $\Delta\Delta G$ were −3.0°C and −0.7 kcal/mol for the entire dataset. Pro mutants in all types of secondary structure were on average found to be destabilizing (Table VI) except for Pro mutations at the N-terminal residue of the helix, which showed a slight stabilization. In contrast, the mutants characterized in the present study, on average show a small increase in thermal stability. This is probably because the selection criteria used to choose sites to be mutated in the present study ensured that in most cases the Pro residue could be accommodated without loss of hydrogen bonding and without unfavorable steric overlaps with neighboring residues. However, the magnitude of the observed stabilization is smaller than that predicted from entropic considerations alone.[40] This is possibly either because of conformational restrictions in the unfolded state, or because the mutated Pro residue is not as well packed as the original WT residue, even at surface exposed sites.

CONCLUSIONS

Pro was introduced at multiple sites in four different proteins. At room temperature, protein stabilities were either slightly decreased or remained unchanged. At

higher temperatures, the increases in thermal stability observed with single Pro mutants in the best cases are quite modest and are significantly smaller than those observed with some engineered disulfides.[46] However, by introducing multiple Pro residues at well separated locations, it may be possible to engineer larger changes in thermal stability. Future studies are required to examine the additivity properties of these mutations. The data were analyzed to suggest guidelines for selection of structurally compatible sites for introduction of Pro in proteins. At such sites the ϕ value should be within 30° of −63° (the average value for Pro) with larger deviations permissible close to chain termini. Pro is well tolerated in turns and coils as well as at the N termini of α-helices and β-strands. In addition, the WT amide proton should not be involved in a main chain hydrogen bond, and the sidechain of the WT residue should not be involved in significant, local stabilizing interactions.

ACKNOWLEDGMENTS

The authors thank Drs S. Mowbray and L. Luck for expression plamids for WT RBP and LIVBP, respectively. The *E. coli* strain Mri7 was obtained from the *E. coli* Genetic Stock Center, Yale University.

REFERENCES

1. Strickler SS, Gribenko AV, Gribenko AV, Keiffer TR, Tomlinson J, Reihle T, Loladze VV, Makhatadze GI. Protein stability and surface electrostatics: a charged relationship. Biochemistry 2006; 45:2761–2766.
2. Grimsley GR, Shaw KL, Fee LR, Alston RW, Huyghues-Despointes BM, Thurlkill RL, Scholtz JM, Pace CN. Increasing protein stability by altering long-range coulombic interactions. Protein Sci 1999;8:1843–1849.
3. Ohmura T, Ueda T, Ootsuka K, Saito M, Imoto T. Stabilization of hen egg white lysozyme by a cavity-filling mutation. Protein Sci 2001;10:313–320.
4. Ishikawa K, Nakamura H, Morikawa K, Kanaya S. Stabilization of *Escherichia coli* ribonuclease HI by cavity-filling mutations within a hydrophobic core. Biochemistry 1993;32:6171–6178.
5. Langsetmo K, Fuchs JA, Woodward C. The conserved, buried aspartic acid in oxidized *Escherichia coli* thioredoxin has a pKa of 7.5. Its titration produces a related shift in global stability. Biochemistry 1991;30:7603–7609.
6. Dani VS, Ramakrishnan C, Varadarajan R. MODIP revisited: re-evaluation and refinement of an automated procedure for modeling of disulfide bonds in proteins. Protein Eng 2003;16:187–193.
7. Matsumura M, Signor G, Matthews BW. Substantial increase of protein stability by multiple disulphide bonds. Nature 1989;342: 291–293.
8. MacArthur MW, Thornton JM. Influence of proline residues on protein conformation. J Mol Biol 1991;218:397–412.
9. Yutani K, Hayashi S, Sugisaki Y, Ogasahara K. Role of conserved proline residues in stabilizing tryptophan synthase α subunit: analysis by mutants with alanine or glycine. Proteins 1991;9:90–98.
10. Allen MJ, Coutinho PM, Ford CF. Stabilization of *Aspergillus awamori* glucoamylase by proline substitution and combining stabilizing mutations. Protein Eng 1998;11:783–788.
11. Bogin O, Peretz M, Hacham Y, Korkhin Y, Frolow F, Kalb AJ, Burstein Y. Enhanced thermal stability of *Clostridium beijerinckii* alcohol dehydrogenase after strategic substitution of amino acid residues with prolines from the homologous thermophilic *Thermoanaerobacter brockii* alcohol dehydrogenase. Protein Sci 1998;7:1156–1163.
12. Herning T, Yutani K, Inaka K, Kuroki R, Matsushima M, Kikuchi M. Role of proline residues in human lysozyme stability: a scanning calorimetric study combined with X-ray structure analysis of proline mutants. Biochemistry 1992;31:7077–7085.
13. Li Y, Reilly PJ, Ford C. Effect of introducing proline residues on the stability of *Aspergillus awamori*. Protein Eng 1997;10:1199–1204.
14. Nakamura S, Tanaka T, Yada RY, Nakai S. Improving the thermostability of *Bacillus stearothermophilus* neutral protease by introducing proline into the active site helix. Protein Eng 1997; 10:1263–1269.
15. Ferrer-Costa C, Orozco M, de la Cruz X. Characterization of disease-associated single amino acid polymorphisms in terms of sequence and structure properties. J Mol Biol 2002;315:771–786.
16. Chasman D, Adams RM. Predicting the functional consequences of non-synonymous single nucleotide polymorphisms: structure-based assessment of amino acid variation. J Mol Biol 2001;307:683–706.
17. Ho SN, Hunt HD, Horton RM, Pullen JK, Pease LR. Site-directed mutagenesis by overlap extension using the polymerase chain reaction. Gene 1989;77:51–59.
18. Beena K, Udgaonkar JB, Varadarajan R. Effect of signal peptide on the stability and folding kinetics of maltose binding protein. Biochemistry 2004;43:3608–3619.
19. Ganesh C, Shah AN, Swaminathan CP, Surolia A, Varadarajan R. Thermodynamic characterization of the reversible, two-state unfolding of maltose binding protein, a large two-domain protein. Biochemistry 1997;36:5020–5028.
20. Prajapati RS, Lingaraju GM, Bacchawat K, Surolia A, Varadarajan R. Thermodynamic effects of replacements of Pro residues in helix interiors of maltose-binding protein. Proteins 2003;53: 863–871.
21. Lopilato JE, Garwin JL, Emr SD, Silhavy TJ, Beckwith JR. D-ribose metabolism in *Escherichia coli* K-12: genetics, regulation, and transport. J Bacteriol 1984;158:665–673.
22. Ames GF, Prody C, Kustu S. Simple, rapid, and quantitative release of periplasmic proteins by chloroform. J Bacteriol 1984;160: 1181–1183.
23. Ghoshal AK, Swaminathan CP, Thomas CJ, Surolia A, Varadarajan R. Thermodynamic and kinetic analysis of the *Escherichia coli* thioredoxin-C′ fragment complementation system. Biochem J 1999;339(Part3):721–727.
24. Pace CN, Vajdos F, Fee L, Grimsley G, Gray T. How to measure and predict the molar absorption coefficient of a protein. Protein Sci 1995;4:2411–2423.
25. Holmgren A, Reichard P. Thioredoxin 2: cleavage with cyanogen bromide. Eur J Biochem 1967;2:187–196.
26. Lee H, Chi SW, Kang M, Baek K, Kim H. Stability and folding of precursor and mature tryptophan-substituted ribose binding protein of *Escherichia coli*. Arch Biochem Biophys 1996;328:78–84.
27. Chakrabarti A, Srivastava S, Swaminathan CP, Surolia A, Varadarajan R. Thermodynamics of replacing an α-helical Pro residue in the P40S mutant of *Escherichia coli* thioredoxin. Protein Sci 1999;8:2455–2459.
28. Schellman JA. The thermodynamic stability of proteins. Annu Rev Biophys Biophys Chem 1987;16:115–137.
29. Sharff AJ, Rodseth LE, Spurlino JC, Quiocho FA. Crystallographic evidence of a large ligand-induced hinge-twist motion between the two domains of the maltodextrin binding protein involved in active transport and chemotaxis. Biochemistry 1992; 31:10657–10663.
30. Otwinowski Z, Minor W. Processing of X-ray diffraction data collected in oscillation mode. Methods Enzymol 1997;276:307–326.
31. Duan X, Hall JA, Nikaido H, Quiocho FA. Crystal structures of the maltodextrin/maltose-binding protein complexed with reduced oligosaccharides: flexibility of tertiary structure and ligand binding. J Mol Biol 2001;306:1115–1126.
32. Collaborative Computational Project. The CCP4 suite: programs for protein crystallography. Acta Crystallogr D Biol Crystallogr 1994;50:760–763.
33. Brunger AT, Adams PD, Clore GM, DeLano WL, Gros P, Grosse-Kunstleve RW, Jiang JS, Kuszewski J, Nilges M, Pannu NS, Read RJ, Rice LM, Simonson T, Warren GL. Crystallography & NMR system: a new software suite for macromolecular structure determination. Acta Crystallogr D Biol Crystallogr 1998; 54(Part5):905–921.

34. Ramachandran GN, Ramakrishnan C, Sasisekharan V. Stereochemistry of polypeptide chain configurations. J Mol Biol 1963;7:95–99.
35. Ramachandran GN, Sasisekharan V. Conformation of polypeptides and proteins. Adv Protein Chem 1968;23:283–438.
36. Ramakrishnan C, Ramachandran GN. Stereochemical criteria for polypeptide and protein chain conformations. II. Allowed conformations for a pair of peptide units. Biophys J 1965;5:909–933.
37. Greene RF, Jr, Pace CN. Urea and guanidine hydrochloride denaturation of ribonuclease, lysozyme, α-chymotrypsin, and β-lactoglobulin. J Biol Chem 1974;249:5388–5393.
38. Pfeil W, Privalov PL. Thermodynamic investigations of proteins. III. Thermodynamic description of lysozyme Biophys Chem 1976; 4:41–50.
39. Reimer U, Scherer G, Drewello M, Kruber S, Schutkowski M, Fischer G. Side-chain effects on peptidyl-prolyl cis/trans isomerisation. J Mol Biol 1998;279:449–460.
40. Matthews BW, Nicholson H, Becktel WJ. Enhanced protein thermostability from site-directed mutations that decrease the entropy of unfolding. Proc Natl Acad Sci USA 1987;84:6663–6667.
41. Pappu RV, Srinivasan R, Rose GD. The flory isolated-pair hypothesis is not valid for polypeptide chains: implications for protein folding. Proc Natl Acad Sci USA 2000;97:12565–12570.
42. Hardy F, Vriend G, Veltman OR, van der Vinne B, Venema G, Eijsink VG. Stabilization of *Bacillus stearothermophilus* neutral protease by introduction of prolines. FEBS Lett 1993;317:89–92.
43. Muslin EH, Clark SE, Henson CA. The effect of proline insertions on the thermostability of a barley α-glucosidase. Protein Eng 2002;15:29–33.
44. Stewart RJ, Varghese JN, Garrett TP, Hoj PB, Fincher GB. Mutant barley (1–≫3,1–≫4)-β-glucan endohydrolases with enhanced thermostability. Protein Eng 2001;14:245–253.
45. Bava KA, Gromiha MM, Uedaira H, Kitajima K, Sarai A. ProTherm, version 4.0: thermodynamic database for proteins and mutants. Nucleic Acids Res 2004;32:D120–D121.
46. Chakraborty K, Thakurela S, Prajapati RS, Indu S, Ali PS, Ramakrishnan C, Varadarajan R. Protein stabilization by introduction of cross-strand disulfides. Biochemistry 2005;44:14638–14646.